Analysis of powder flow and in-system rheology in a horizontal convective mixer with reclining blades

Léonard Legoix, Cendrine Gatumel, Mathieu Milhé, Henri Berthiaux

Analysis of powder flow and in-system rheology in a horizontal convective mixer with reclining blades

Léonard Legoix, Cendrine Gatumel, Mathieu Milhé, and Henri Berthiaux

Ecole des Mines Albi, RAPSODEE Centre, CNRS UMR 5302, Albi, France

ABSTRACT

A prototypal convective mixer, designed and built for this work, allows investigating powder rheology under various geometrical configurations. The configuration chosen here is a horizontal vessel with four rectangular blades. Two blade inclinations (0–33°) and three filling ratios are studied for two powders of different kind: a free-flowing powder (semolina) and a cohesive powder (lactose). For the smaller agitation speeds, the flow regime of the powder is rolling and is characterized by surface powder avalanches. For greater agitation speeds, the flow regime is cataracting, with particle projections that follow the blade movement. These flow regimes are identified for both powders and do not depends on the filling ratio. Rheological measurements evidence that the blade inclination has little impact on the mechanical power needed to stir the free-flowing powder. It has an impact observable on cohesive powders, especially for high filling ratios. A correlation between the power number and the Froude number is established and compared to previous results obtained on a different technology. It is of the form: $N_p = a.F_r^b$. The dependencies of the coefficients a and b on the powder type and on the flow regime are quantified.

KEYWORDS

Cohesive powders; convective blender; flow regimes; powder mixing; rheology

Introduction

Powder blending is a key operation for many industries, such as pharmaceutical, agro-food industries, construction, or metallurgy. Technologies to mix powders can be divided into two groups: tumbling blenders for which the rotation of the vessel provokes the motion and subsequent mixing of the powder bed, and convective blenders for which powder is put into motion by the action of an impeller inside a fixed tank. For free-flowing powders of different particle sizes, the avalanching created by most of tumbling blenders enhances segregation (Moakher, Shinbrot, and Muzzio 2000), as well as it favors the aggregation of the particles for cohesive systems. Despite some difficulties that may arise in their cleaning procedures, the use of convective blenders is now generalized in the industry, because of their polyvalence to process any kind of systems. In the case of cohesive systems, they are the most recognized alternative for their ability to break agglomerates and create a better mixture at the smallest scale.

Convective blenders can be operated either in continuous or batch regimes, the first one gaining more ground every day, as a way to enhance productivity in factories. However, batch mixing processes are still the rule, because of their reliability to assess batches of products. For years, batch convective mixers have been designed through a simple principle: impellers mounted on a horizontal shaft rotating at a fixed speed, the main technology being the Lödige® mixer. This blender has been studied through experiments and simulations with powders of different shapes (Laurent and Cleary 2012; Cleary 2013). Its impellers are designed like a ploughshare that penetrates into the powder bed progressively and creates side flows. Other complex designs of impellers exist like ribbons or screws, but blades are simpler and processed in different technologies of powder blending, like high-shear mixers (Knight et al. 2001) or the Triaxe® planetary blender (Demeyre 2007).

In the scientific literature, several papers studied the action of various blade systems on the powder with a physical approach, so as to get a better understanding of powder flow at the smallest scale. The action of a single flat rectangular blade over a granular bed has been studied since the 1960s in various works, through camera observations and torque measurements (Bagster and Bridgewater 1969; Bagster and Bridgewater 1967). More recently, it has been investigated with the help of high-velocity camera acquisition, and analysis by Particle Image Velocimetry (Radl et al. 2012), as well as modeling by discrete element method (Chandratilleke, Yu, and Bridgwater 2012; Siraj 2014). These studies were focused on the influence of different parameters on rheology, such as blade angle or shape, blade speed, or blade position inside the powder bed. They proved that a recirculation zone on the surface in front of the blade exists and its size depends on blade position, angle, and velocity. This recirculation is a helpful mechanism in the general blending process. These fundamental studies that are essential to understand how powder moves around a moving obstacle are of limited

CONTACT Henri Berthiaux henri.berthiaux@mines-albi.fr Ecole des Mines Albi, RAPSODEE Centre, CNRS UMR 5302, Campus Jarlard, Route de Teillet, Albi 81000, France.

Color versions of one or more of the figures in the article can be found online at www.tandfonline.com/upst.

interest since they concern the flow over a blade in two dimensions surrounded by transparent lateral walls along the flow direction. Indeed, this is not the case in a blending process that uses the motion of numerous impellers that can cover the vessel in the three dimensions of space. This is the reason why mixing or rheological studies performed during processing can add valuable information that can be applied directly in the industry.

At the level of the process, research works have been concerned with horizontal convective blenders (Malhotra et al. 1988; Malhotra and Mujumdar 1990; Malhotra, Mujumdar, and Miyahara 1990a; Malhotra, Mujumdar, and Okazaki 1990b; Laurent and Bridgwater 2002) and also vertical convective blenders (Makishima and Shirai 1968; Zhou et al. 2004; Conway et al. 2005; Chandratilleke et al. 2009; Remy et al. 2010; Remy, Khinast, and Glasser 2011; Halidan et al. 2014; Havlica et al. 2015). These papers provide valuable information about powder flow, rheology, and mixing kinetics. However, they are usually confined to free-flowing systems and mixers operating in single flow regimes.

The existence of different flow regimes and their impact on the prevalence of certain mixing mechanisms and mixing kinetics has been studied for tumbling blenders (Mellmann 2001 and Mayer-Laigle 2012). It has been found that their knowledge is essential in the scaling-up procedure of mixers, as dynamics or kinematics similarities are never considered in the conception of powder mixers. The present work aims at identifying and studying flow regimes in convective blenders and can be placed in the continuity of these previous studies. For this, a transparent polyvalent prototype equipped with a torque measurement system has been designed. It aims at identifying the impact of different geometrical parameters, such as the number of blades, their inclination, the vessel's volume, the positioning of the blade system inside the vessel, and the inclination of the tank itself. Different kind of powders can be studied according to their rheological characterization (free-flowing or cohesive) that can be verified in situ. This work is restricted to the horizontal position of the mixer with four reclining blades mounted on the shaft and is divided into three main parts. First, powder motion and flow will be characterized through simple observation in order to identify the flow regimes in the blender. Then, a focus will be made on the mechanical power required to stir powders of different types, with different blade angles and different filling ratios through process rheometry. Finally, a general method to express the rheological measurements will be suggested for scale-up calculations.

Materials and methods

Powders considered

Two powders have been studied: a free-flowing one and a cohesive one. The free-flowing powder is fine semolina (Le Renard) and the cohesive powder chosen is lactose (Granulac140). Both particles are of polygonal shape, as shown by SEM pictures in Figure 1.

Table 1 shows the main properties of these two powders, d_{50} being the median diameter measured by LASER diffraction

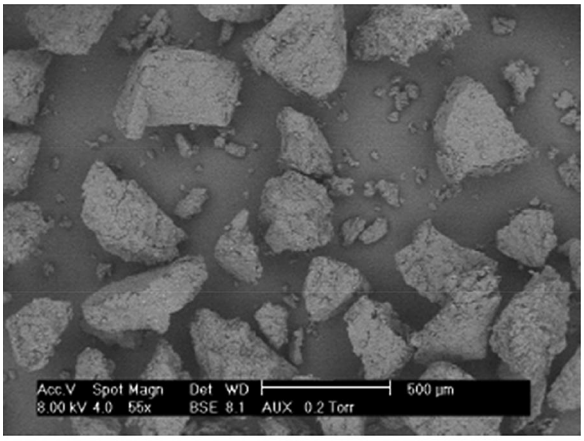

(a)

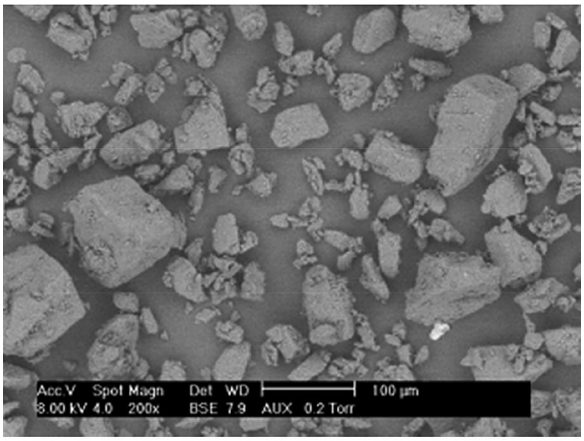

(b)

Figure 1. SEM pictures of semolina (a) and lactose (b).

with a Mastersizer3000 (Malvern) under an air pressure of 3.5 bars. The particle true density ρ_p has been measured thanks to an Accumulator® Pyc 1330 (Micromeritics) with the 10 cm^3 cell. The bulk and tapped densities ρ_b and ρ_t have been measured with a volumenometer (Erweka®) for a powder mass of 110 g. The tapped density has been measured after 1000 taps, which is enough to be sure that the powder cannot be more packed by the apparatus since the volume stabilizes around 300 taps. The Carr Index for semolina is smaller than 15%, which makes it an easy flowing powder. For lactose, the Carr Index is greater than 15% which is characteristic for powders that do not flow easily (Leturia et al. 2014). This attests that semolina can be considered as a free-flowing powder, whereas lactose is a cohesive system.

Convective blender prototype

A prototypal convective mixer has been designed and built in order to get a better understanding of powder flow regimes

Table 1. Powder properties measured.

Powder	d_{50} (µm)		d_{10} (µm)		d_{90} (µm)		ρ_p (kg.m^{-3})	ρ_b (kg.m^{-3})	ρ_t (kg.m^{-3})	CI (%)
Semolina	328	330	208	207	496	492	1463	679	720	5.8
Lactose	62	62	17	17	144	144	1533	661	795	16.9

In bold: Particle size values after agitation showing the absence of attrition.

and governing mechanisms under very different geometrical configurations. The cylindrical tank, delimited by two lateral walls, is made of PMMA because of its mechanical resistance and so as to observe the progression of the mixing process (Figure 2). The vessel diameter is 24 cm, blade-to-wall distance is 1 mm, and blade width is 6 cm. The rotational speed can be varied between 2 and 20 rad.s^{-1} thanks to a gear-motor. A torquemeter allows recording the motor torque between 0 and 15 Nm. Rotational speed and torque are acquired thanks to a Labview® program that records the torque at 1 Hz. The powder can be loaded thanks to a rectangular aperture in the cylinder.

The mixer has been conceived as a multifunctional tool, so as to study the influence of four parameters: the number of blades, the blade angle, the vessel angle, and the position of the walls with respect to the stirring system.

Blades

Between 1 and 4 blades can be mounted on the shaft, in any of the four locations available as shown in Figure 3. The distance between each blade tip and the vessel is about 1 mm. The blade angle α with respect to the shaft can also be adjusted blade by blade, between 0° and 180° (Figure 3). In the present study, the four blades will be mounted on the shaft, all at the same angle. Two angles will be studied: 0° and 33°. For $\alpha = 0°$, the blades will be qualified as "straight blades" and for $\alpha = 33°$, the blades will be qualified as "reclined blades".

Vessel

The vessel angle can be adjusted with the spinning table on which the vessel, the torquemeter, and the motor are fixed (Figure 4). The vessel angle can be chosen between $-90°$ and 90°, with the angle orientation as shown in Figure 4. In this study, the vessel angle will be fixed at 0°, placing therefore the mixer in the horizontal position.

Walls

The powder remains inside the cylindrical vessel thanks to two disk-shaped lateral walls. Each wall is equipped with O-rings,

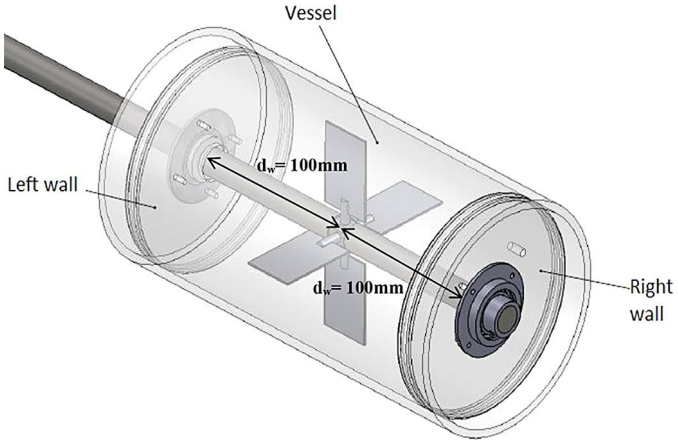

Figure 2. Blending prototype showing the four rectangular blades and the adjustable lateral walls.

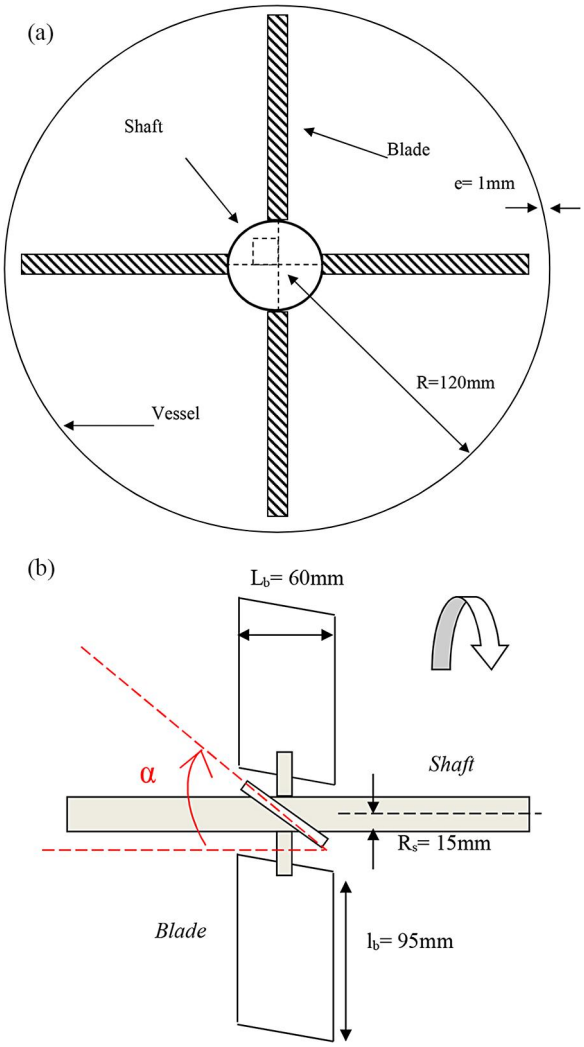

Figure 3. The four blade positions in the polyvalent bladed blender, side view (a) and blade angle definition (b).

giving a good sealing of the vessel to fine powders. They both can be placed everywhere on the shaft on each parts of the blades, so that the agitation device is not necessarily centered between these walls (Figure 5). For this work, the blades are centered at a wall-blade distance of 10 cm.

Experimental procedure

As stated above, the torquemeter allows performing in-process rheometry by measuring the torque exerted on the shaft during stirring. Each experiment begins by running the blades 5 min at a speed of 8 rad.s^{-1} in the empty vessel. Torques are then measured at a speed increasing from 3 to 18 rad.s^{-1} with a 3 rad.s^{-1} step. For each speed, the agitation is maintained

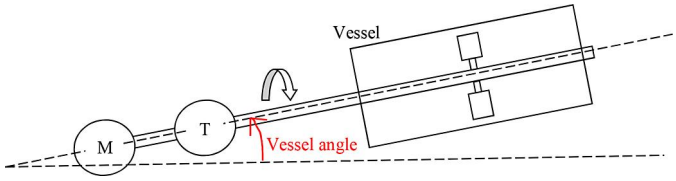

Figure 4. Vessel inclination (M: motor, T: torquemeter).

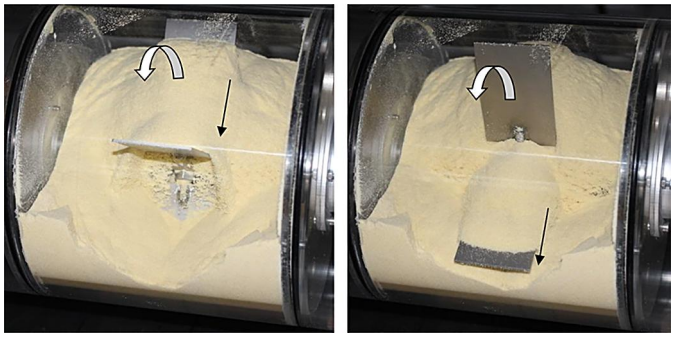

Figure 5. Observation of the rolling flow regime for semolina inside the convective blender equipped with straight blades, at $F_r = 0.1$ and $f = 0.63$. The white and black arrows show, respectively, blade rotation and powder motion.

during 5–10 min to be sure that the torque is stabilized, after which its mean value is calculated over 1 min and will be considered as the recorded empty torque. Then, the vessel is filled with the powder studied and after a conditioning step that lasts 5 min at 8 rad.s^{-1}, the same torque measurement procedure is repeated. For all studies, three filling ratios f are investigated: 0.42, 0.63, and 0.83. These filling ratios are calculated as follows:

$$f = \frac{m_p}{\rho_b V_{\text{tank}}}, \tag{1}$$

where ρ_b (kg.m^{-3}) is the bulk density of the powder, m_p (kg) is the mass of powder, and V_{tank} (m^3) is the volume of the blender, which is about 8.85 l. The power consumption can be calculated as

$$P = \omega\left(T_f - T_0\right), \tag{2}$$

where ω (rad.s^{-1}) is the rotational speed of the blade, T_0 (N.m) is the empty torque, and T_f (N.m) is the torque with filled vessel. Dimensional analysis of this process leads to the definition of different numbers, such as the Froude number F_r and the power number N_p. These two numbers can be calculated as

$$F_r = \frac{R.\omega^2}{g}, \tag{3}$$

$$N_p = \frac{P}{\rho_b \omega^3 R^5}, \tag{4}$$

where g (m.s^{-2}) is the standard gravity, ω (rad.s^{-1}) is the rotational speed of the blade, R (m) is the radius of the blade, ρ_b (kg.m^{-3}) is the bulk density of the powder, and P (W) is the power consumption. This approach is useful for scale-up calculations, or to predict power consumption at industrial scale, thanks to lab-scale or pilot-scale experiments that require less powder and consume less energy. With the rotational speeds considered in this work, the Froude numbers involved are 0.1, 0.4, 1.0, 1.8, 2.8, and 4.0. The different process parameters of each experiment are provided in Table 2. For these 12 combinations of powder cohesion, blade inclination, and filling ratios, the six rotational speeds listed above, ranging from 3 to 18 rad.s^{-1}, will be studied.

Table 2. Powder and process parameters investigated.

Powder	Semolina–lactose
Blade angle (°)	0–33
f	0.42–0.63–0.83
ω (rad.s^{-1})	3–6–9–12–15–18

Flow observations have been performed using a Canon 650D camera with an 18–55 mm lens. The same rotational speeds and filling ratios are studied as for rheology measurements. An exposure time of the digital sensor of 5 ms is used, which is the greatest duration available with the photoflash for this device. This is fast enough to strap up the powder flow, even for the greatest rotational speeds, which is useful to observe flow regimes. All the pictures are taken in the front view of the blender, meaning that the vector of the angular speed goes from the left to the right. The direction of the rotation is reminded on each figure with a flat white arrow, while black arrows highlight powder flows.

Attrition and temperature

Attrition and temperature elevation have been measured to ensure that powder properties do not change during and after the mixing operation. A size distribution analysis has been made after one typical series of measures with various rotational speeds (3, 6, 9, 12, 15, and 18 rad.s^{-1}) at 10 min of agitation for each speed. The powder was sampled inside the zone agitated by the blades, the motor being turned off. The particle size distributions described by the three characteristic diameters d_{10}, d_{50}, and d_{90} are almost the same.

The temperature was measured near the blades just after the stirring operation described before. The ambient temperature of the laboratory was about 22°C and the powder temperature reached 27°C. This observable temperature increase is not enough to influence significantly the torque exerted on blades.

Identification of powder flow regimes

Free-flowing material flow

Qualitative observations of different flow regimes in the agitated zone of the blender were made thanks to the pictures taken with the camera. Two main flow regimes have been distinguished for the free-flowing particulate system: the rolling regime and the cataracting regime. These names are given in analogy with those employed for tumbling blenders operating with free-flowing material, as in the classification given by Mellmann (2001). This can be adapted for the convective blender, since the powder flow has some similarities. Concerning the rolling regime, the powder follows the walls or the blades until it reaches a vertical position, and then rolls down by avalanches. At higher speeds, a cataracting regime can be observed. Once the particles are not in contact with the walls or the blades, they follow the same trajectory and do not roll by avalanching. This is characterized by projections of particles in the air.

The Froude number that compares the centrifugal force with gravity helps characterizing the flow regime that takes place in the blender. Knowing the rotational speed ω (rad.s^{-1}) and the distance R from the center of the shaft to the blade tip, the maximal centrifugal force provided by

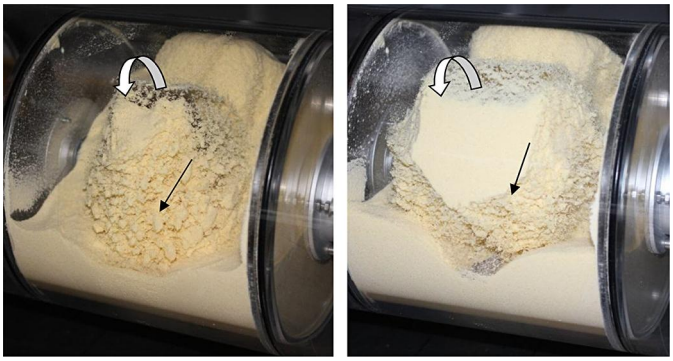

Figure 6. Centrifuging flow regime for semolina inside the convective blender equipped with straight blades, at $F_r = 1.0$ and $f = 0.63$ (left) and at $F_r = 1.8$ $f = 0.83$ (right).

blades can be calculated and divided by the standard gravity g (Equation 3). Pictures taken while semolina is stirred show that when the Froude number is smaller than 1, the flow regime is rolling. This can be observed especially when the blade goes from a horizontal position to a vertical position, and is off the powder bed (Figure 5). The powder taken by a blade rolls by avalanches to the next blade, since the centrifugal force is less influent than gravity. Conversely, when the Froude number is greater than 1, the powder flow regime is cataracting. This is easy to observe since the powder is projected by the blade instead of rolling in front of it (Figure 6).

For this flow regime determination, observations are characteristic of the flow in front of the blades, at the free-surface level. Indeed, for a filling ratio of 0.42, 0.63, and 0.83, a Froude number of 1 is always the border of a flow regime change (Table 3).

The influence of blade angle has also been observed. The same conclusions as for straight blades can be drawn: for a Froude number smaller than 1, the flow regime is rolling and when it is greater than 1, the flow regime is cataracting. However, if the blade angle chosen here does not change the flow regime, the powder flow is obviously different in other ways. For instance, an asymmetric axial flow has been identified. This can be observed in the front views of Figure 7, in which the powder moves axially from the right to the left of the vessel: blades throw the powder along a preferential direction, depending on the blade inclination. The pictures taken with reclined blades show that when the Froude number is too small, the powder can fall on the next blade, and part of it rolls down to the right. For higher blade speeds, with a Froude number greater than 1, the lateral projection of powder is more efficient since all the powder moved by the blades goes to the same lateral way, on the left. These qualitative observations highlight the central role of F_r in the transport mechanisms involved in the stirring of free-flowing powders.

Table 3. Map of flow regimes for semolina agitation with the convective blender.

f \ F_r	0.1	0.4	1.0	1.8	2.8	4.0
0.42	Rolling	Rolling	Cataracting	Cataracting	Cataracting	Cataracting
0.63	Rolling	Rolling	Cataracting	Cataracting	Cataracting	Cataracting
0.83	Rolling	Rolling	Cataracting	Cataracting	Cataracting	Cataracting

Figure 7. Rolling flow regime (left) and cataracting flow regime (right) for semolina inside the convective blender equipped with reclined blades.

Cohesive powder flow

Experiments carried out with lactose show the same behavior to what concerns Froude numbers. A rolling regime and a cataracting regime can be identified when the Froude number is smaller or greater than 1, respectively. As for semolina, the filling ratio has no influence on these regimes.

However, a difference between semolina and lactose flow can be detected in the rolling regime. For semolina, all the powder carried by blades rolls down, but for lactose, the powder avalanching occurs by blocks that fall one after the other. This is due to cohesion forces between particles that do not allow them to fall separately (Figure 8). Concerning reclined blades, as for semolina, the same flow regimes of rolling and cataracting are observed, with an axial asymmetry of the flow (Figure 9). Concerning the rolling regime, the avalanche on the next blade of a part of the powder swept by the previous blade is also observed.

In-mixer rheology

Power consumption has been recorded for the six rotational speeds ω, the three filling ratios f studied, and the two particulate systems. Each experiment has been repeated twice to evaluate measurements repeatability. The deviation of the power P_1 and P_2 between two identical experiments can be calculated as

$$\Delta P = \frac{|P_1 - P_2|}{P_1} \times 100. \quad (5)$$

The data are reproducible for semolina with straight blades, with ΔP values smaller than 8% (Table 4). When blades are reclined, data are less reproducible for semolina with values

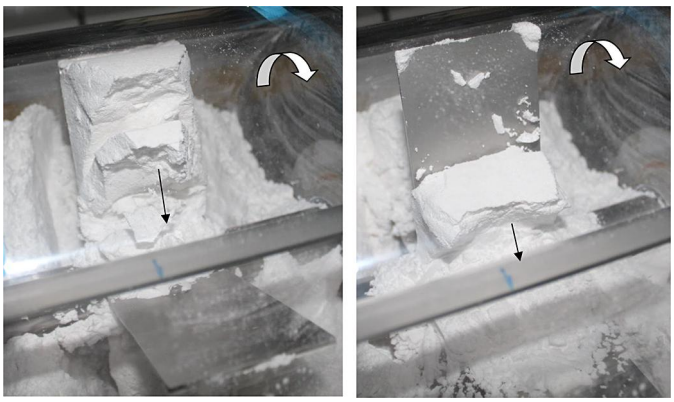

Figure 8. Consecutive falling of lactose powder by blocks, at $F_r = 0.1$ and $f = 0.42$, straight blades.

Figure 9. Rolling flow regime (left) and cataracting flow regime (right) of lactose inside the convective blender equipped with reclined blades.

Table 4. Deviations of the power measurements (%).

Powder	Blades	f	3 rad.s^{-1}	6 rad.s^{-1}	9 rad.s^{-1}	12 rad.s^{-1}	15 rad.s^{-1}	18 rad.s^{-1}
Semolina	Straight	0.42	6.5	7.2	7.4	5.1	1.1	1.8
		0.63	3.2	3.7	0.3	1.1	1.3	1.6
		0.83	0.4	4.2	2.5	2.0	0.6	0.6
	Reclined	0.42	13.5	16.2	20.1	2.3	4.9	4.8
		0.63	7.4	4.9	3.7	0.4	1.5	1.7
		0.83	7.1	7.0	3.6	15.4	14.3	0.1
Lactose	Straight	0.42	7.7	8.4	8.3	0.8	10.9	11.2
		0.63	20.9	27.6	27.2	19.7	19.6	4.4
		0.83	17.9	45.1	42.0	18.4	15.8	8.6
	Reclined	0.42	11.1	7.7	57.0	28.2	30.4	11.8
		0.63	10.0	3.8	3.1	2.1	3.6	3.9
		0.83	4.4	5.6	20.3	12.8	11.2	6.8

comprised between 0.4% and 20.1%. Concerning lactose, values of ΔP can reach 45.1% for straight blades and 57.0% for reclined blades.

Influence of blade inclination

Figure 10(a–c) reports the power consumption of the system for semolina, as a function of the rotational speed of the impeller for the three filling ratios investigated. For all the cases studied, P increases with ω, as expected.

The values of the power are close to each other whether the position of the blades is, especially at small rotational speeds (rolling regime). While promoted by the rotation of the blades, the flow of such particulate systems is still guided by the individual behavior of the particles rather than by the process conditions themselves. As a result, the effect of the blade angle is negligible in this regime. For the two highest speeds considered (cataracting regime), it seems that the power is slightly greater for straight blades than for reclined ones. This may indicate that the more vigorous action of the impeller in the cataracting regime has a deeper impact on powder flow, and

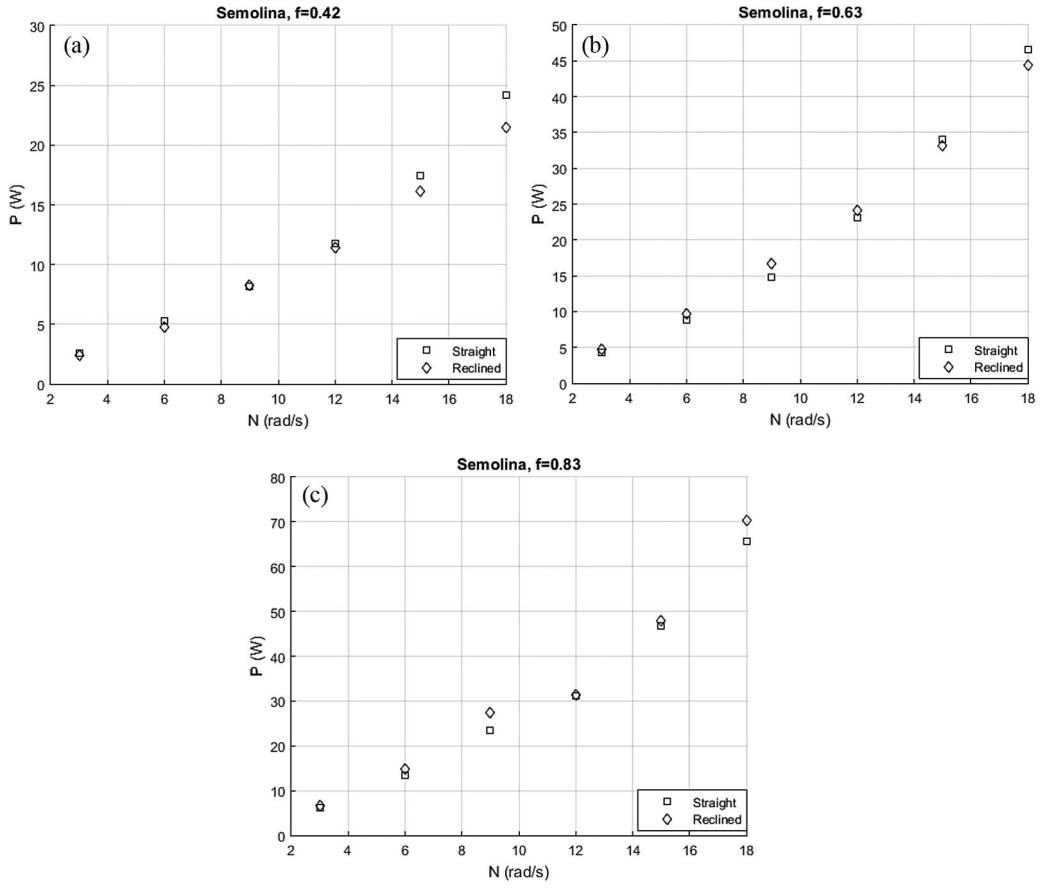

Figure 10. Power requirements to stir semolina in the convective blender according to blade angles, for $f = 0.42$ (a), $f = 0.63$ (b), and $f = 0.83$ (c).

as a result the conditions under which the process runs, such as blade angle, are about to be denoted.

The agitation of lactose has been investigated in the same way, the results being given in Figure 11(a–c). The power consumption is approximately three times smaller for such a cohesive system than for a free-flowing powder. Here, particle–particle interaction helps counteracting particle weight and facilitates the motion of the blades that displaces blocks of powder. Power is also greater for straight blades than for reclined blades, especially for medium-to-high rotational speeds. The presence of a 33° blade angle induces shear of the powder bed in the same direction as that of the blade motion itself. This is more efficient to displace a cohesive system than a flat angle that offers its whole surface to the bulk. With a greater powder mass or filling ratio (i.e., $f = 0.83$), the difference is all the more marked and favors the use of reclined blades to stir cohesive systems in the present horizontal equipment configuration. In the cataracting regime, i.e., for rotational speeds above 15 rad.s^{-1}, the material being pushed as blocks of powder, less energy will be required for reclined than for straight blades.

Influence of filling ratio

The effect of the filling ratio f on the power P can be seen in Figure (12a–b), only for the case of the reclined blades, for both particulate systems.

For the free-flowing powder, the power increases with the filling ratio, whatever the rotational speed considered. As no compaction of such a system is expected, the bulk density does not change and the filling ratio is proportional to the powder weight (Equation 1). Figure 12(a) therefore reflects directly the fact that moving a greater powder mass requires a greater power consumption, in particular if this has to be done at a high speed.

For the cohesive powder, Figure 12(b) reflects a notably different tendency. Indeed, if the power increases between the first two filling ratios (0.42 and 0.63), it decreases for the highest value of f in the majority of the speeds considered. This can be attributed to a local decrease of bulk density of the powder conveyed by the blades or in their vicinity. This is more likely to be noted when the blender is filled and blades are immerged in the system, as the level of stress in the bulk is greater. It can also be noted that blade inclination has a lesser impact on the power than the filling ratio has.

The role of packing state in cohesive powders rheology

It has been observed that both the rotational speed and the filling ratio have an influence on power requirement to stir powders. For semolina, an increase in filling ratio and an increase of rotational speed imply an increase of power consumption. This has also been observed for a 180–250 µm sand in a three-bladed high-shear mixer in the past (Knight et al. 2001). The motion of these systems is mainly driven by friction and their packing state is not influenced significantly by strains applied on the bulk. This means that the average contact number between particles in the bulk does not change

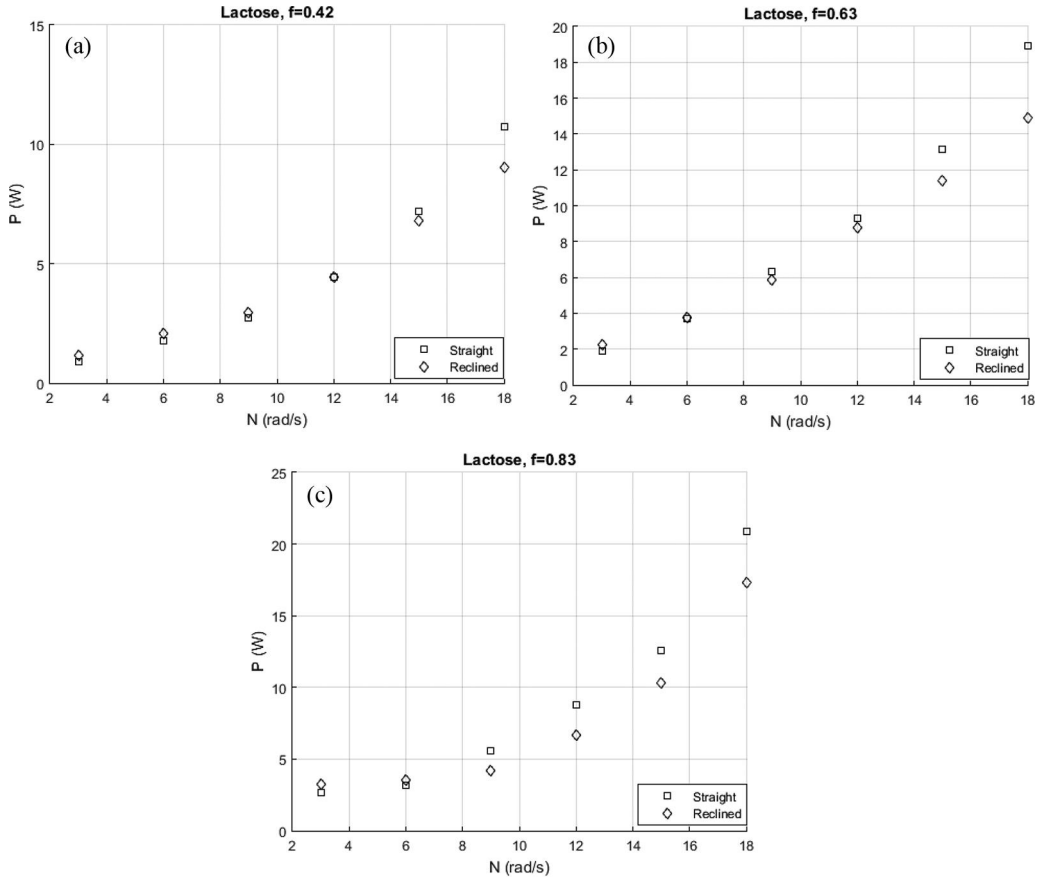

Figure 11. Power requirements to stir lactose in the convective blender according to blade angles, for $f = 0.42$ (a), $f = 0.63$ (b), and $f = 0.83$ (c).

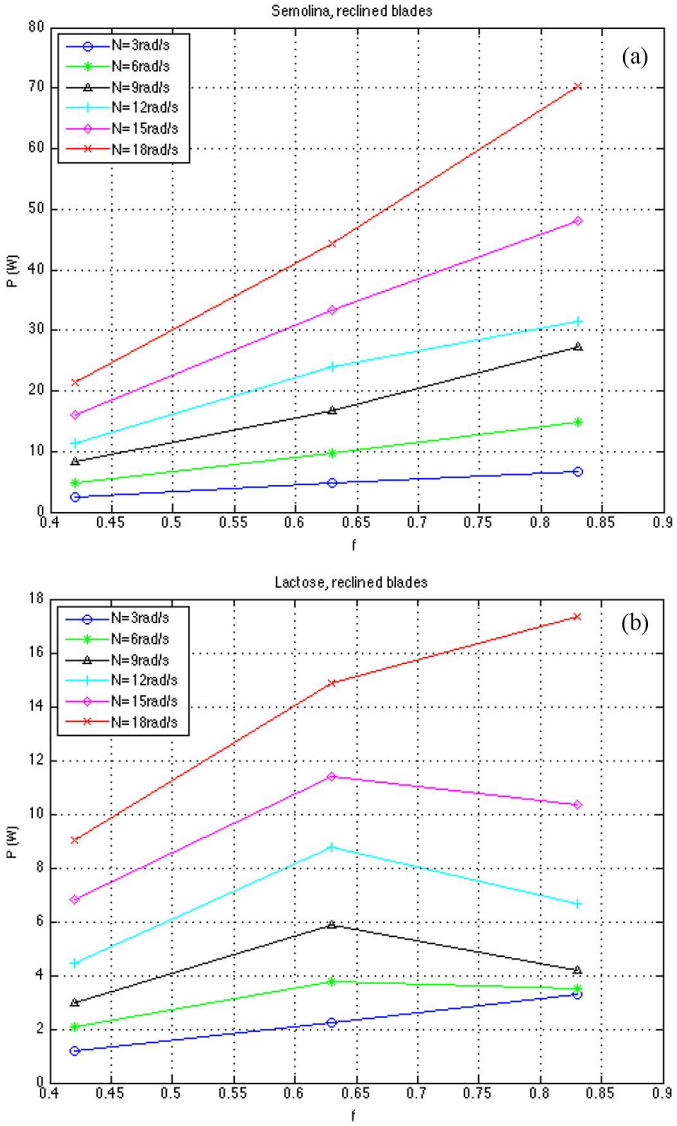

Figure 12. Evolution of power consumption with filling ratio, according to different rotational speeds in the reclined blades case for either semolina (a) or lactose (b).

enough to reduce or increase the influence of friction forces on rheology.

On the contrary, dry cohesive system packing state is more sensitive to the external forces that are applied on the bulk. Two packing states could be observed under small and strong external strength:

1. Under small forces applied, the cohesion force creates a network between particles, in turn creating a porous material demonstrating few inter-particle contacts.
2. On the contrary, when external forces are significant, the air inside these inter-particle pores gets out of the network, increasing the contact numbers between particles. This is the reason why cohesive powders are well known to show a great compressibility (Carr 1965). So like free-flowing powders, the number of contact between particles is important, but the presence of cohesion forces between particles will create a more consolidated particle bed.

This sensibility of the packing state of cohesive powders leads to a different rheological behavior in bladed mixers. For instance, Cavinato et al. observed an increase of impeller torque with filling ratio during the high-shear mixing of a cohesive powder (Cavinato et al. 2013). On the contrary, in our study the value of the torque decreases for most of greater values of filling ratios. This behavior could be explained by a more tied packing of particles for greater values of f (higher than 0.63 in our study), creating more consolidated walls on each lateral side of the blades. As a consequence, the powder forming these vertical walls cannot be in contact with blades by slipping or shearing. Along with this phenomenon, a moving of blocs of particles in front of blades may take place, impeding the creation of a wider contact network of particles, which could exist in free-flowing systems interacting with impeller blades (Boonkanokwong et al. 2016). Therefore, our measurements are in agreement with Cavinato et al., since their range of filling ratio remains relatively small (less than 0.4), and in this range, we also observed an increase of power consumption with filling ratio, which is a behavior similar to that of free-flowing material.

Dimensionless representation

The previous results of power measurements can be represented thanks to dimensionless numbers and correlations. The power is expressed as a power number N_p and the agitation speed as a Froude number F_r. As reported for powder stirring experiments in other studies of convective powder blenders (Knight et al. 2001; André and Demeyre 2012), the typical correlation that links those numbers is of the following form:

$$N_p = a.F_r^b. \tag{6}$$

Establishment of a general correlation

The dimensionless correlation for semolina, with straight blades and a filling of 0.42, is given as an example in Figure 13. In the figure, the logarithms of dimensionless numbers are plotted and linear fits are performed in accordance with Equation (6). This representation shows that for Froude numbers smaller than 1 and for Froude numbers greater than 1, separated correlations should be considered. The slope represents the b coefficient, the intercept being ln (a). The squared coefficients of variation, both greater than 0.99, demonstrate that the power correlation between N_p and F_r is verified. Concerning Froude numbers smaller than 1, meaning that the flow regime is rolling, the coefficient b is close to -1 and the coefficient a has a value of about 0.65. For the cataracting regime, b is close to -0.7 and a value is about 0.63. The coefficient b is therefore significantly different between the two regimes, while the coefficient a can be said to be the same.

Similar correlations have been investigated for the other filling ratios and blade angle, still for the free-flowing material (Table 5). The coefficient b can be said to be independent of the filling ratio, and practically independent of the blade angle in the rolling regime for which its value is close to -1. It is quite sensitive to the flow regime in general,

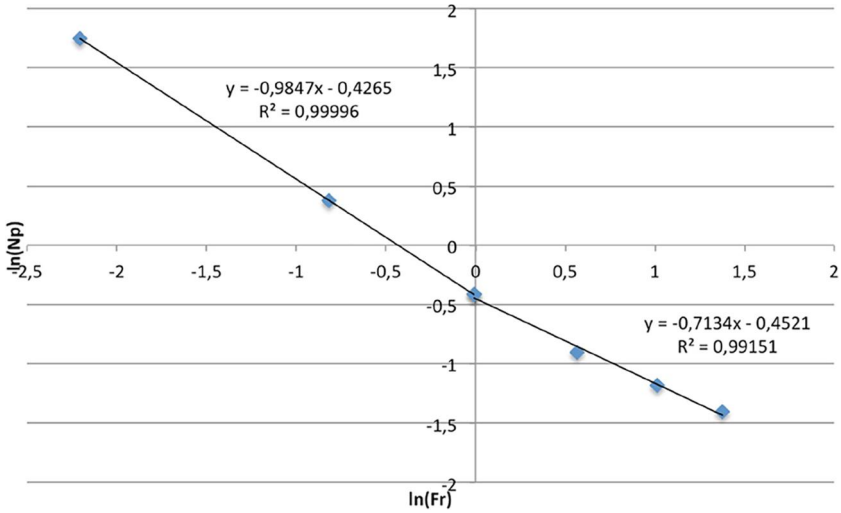

Figure 13. Representation of the correlation between F_r and N_p in the prototype equipped with straight blades, $f = 0.42$, semolina case.

Table 5. Correlation $N_p = a.F_r^b$ coefficients for semolina and lactose agitation with the convective blender.

	Parameters		b		a		R^2	
Powder	Blades	f	Rolling	Cataracting	Rolling	Cataracting	Rolling	Cataracting
Semolina	Straight	0.42	−0.98	−0.71	0.65	0.63	0.999	0.991
		0.63	−0.95	−0.67	1.15	1.18	0.999	0.999
		0.83	−0.89	−0.75	1.84	1.79	0.999	0.978
	Reclined	0.42	−0.92	−0.84	0.64	0.67	0.991	0.992
		0.63	−0.93	−0.79	1.30	1.32	0.998	0.998
		0.83	−0.86	−0.81	2.12	1.99	0.997	0.942
Lactose	Straight	0.42	−0.99	−0.51	0.22	0.22	0.999	0.986
		0.63	−0.96	−0.72	0.50	0.51	0.998	0.991
		0.83	−1.18	−0.58	0.41	0.44	0.985	0.952
	Reclined	0.42	−1.08	−0.69	0.24	0.24	0.999	0.995
		0.63	−1.07	−0.84	0.47	0.49	0.998	0.999
		0.83	−1.40	−0.49	0.33	0.33	0.999	0.935

its value being close to −0.7 in the cataracting regime for straight blades and −0.8 for reclined blades, therefore marking a light impact of the blade angle that may be the transcription of the flow asymmetry that has been qualitatively evidenced. To what concerns coefficient *a*, it is particularly insensitive to the flow regime and to a smaller extent to the blade inclination. Its main acting parameter is undoubtedly the filling ratio that can triplicate its value while *f* is only doubled.

Table 5 also shows similar results for the cohesive material. The coefficient *b* is globally always equal to −1 in the rolling regime, except for the greatest filling ratios and when the blender is equipped with reclined blades (equals to −1.4). In the cataracting regime, while the correlation is of a regular quality, *b* is still close to −0.7 for straight blades and −0.8 for reclined blades. Once again, a filling ratio of 0.83 for reclined blades apparently drives to a different situation. As for semolina, the coefficient *a* is remarkably independent on the flow regime and the blade inclination, its value being the fact of the filling ratio, and the type of material: approximately three times less important for the cohesive powder than for the free-flowing powder.

Globally, it can be said that the coefficient *a* depends on the powder (kind, mass), whereas the coefficient *b* is more sensitive to a change in flow regime.

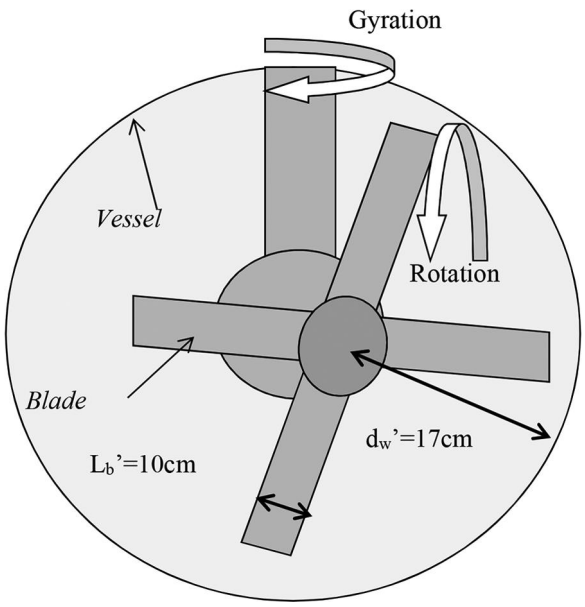

Figure 14. Schematic view of the Triaxe® mixer showing some characteristic lengths.

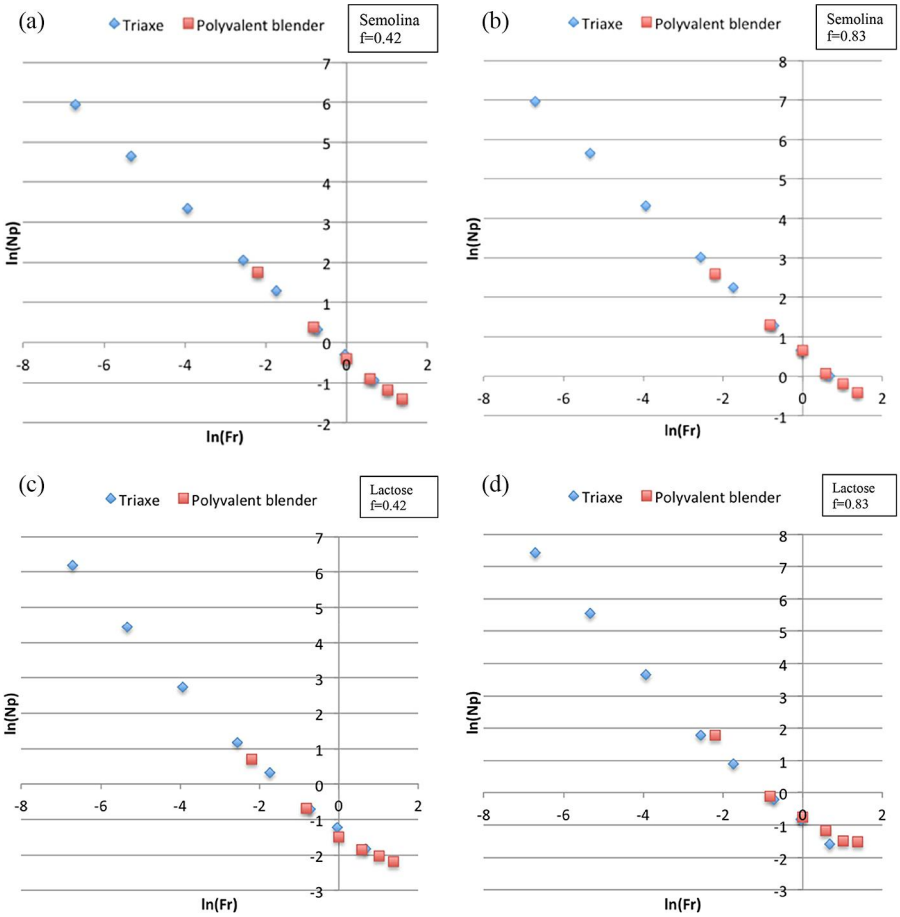

Figure 15. Comparison of the power-law correlations obtained in the Triaxe® blender and the actual prototype: semolina and $f = 0.42$ (a); semolina and $f = 0.83$; lactose and $f = 0.42$; lactose and $f = 0.83$.

Comparison with a planetary blender

The planetary blender Triaxe® has been used in previous work on powder blending and rheology by our research team (Demeyre 2007; André et al. 2014; Legoix et al. 2017). This blender is characterized by a dual movement of rotation and gyration that moves the blade support around the vessel. The suppression of the gyration leads to a movement of the four blades close to the rotation provided by the polyvalent blender studied in this paper. The ratio between the blade width L'_b and the blade-wall distance d'_w is the same as that of the polyvalent blender (Figure 14):

$$\frac{L_b}{L'_b} = \frac{d_w}{d'_w}. \tag{7}$$

As for the horizontal blender, dimensional analysis can be performed for the Triaxe® blender, thanks to the introduction of a power number N_p and a Froude number F_r. These two numbers can be calculated as follows:

$$F_r = \frac{D.\omega_{ra}^2}{2.g}, \tag{8}$$

$$N_p = \frac{P}{\rho_b \omega_{ra}^3 (D/2)^5}, \tag{9}$$

where ω_{ra} (rad.s^{-1}) is the rotational speed of the blades, $D = 0.448$ m is the distance between two opposite blade tips, ρ_b (kg.m^{-3}) is the bulk density of the powder, and P (W) is the power consumption. N_p is plotted against F_r for both equipment in the different operating conditions already studied here (Figure (15a–d)). It must be said that the data are not in the same range of Froude numbers, the Triaxe® covering smaller values while the polyvalent blender covers greater ones. However, there is a partial overlap particularly around $F_r = 1$. Whatever the particulate system considered and the filling ratio, the log–log representation considered in the previous section leads to similar correlations for both technologies. This shows that the polyvalent convective blender designed for this work may be helpful for scale up or power prediction in blenders that cannot be equipped with torquemeters.

Concluding remarks

The polyvalent convective blender, built for this work, allows to investigate in-situ powder rheology induced by blades, and may be helpful in scale-up procedures and understanding of powder flow in different systems. This device has been studied for two powders of different kinds: fine semolina that is free-flowing and lactose, which is cohesive. Flow regimes have been identified for these two powders, three filling ratios (0.42–0.63–0.83) and two blade angles (0–33°). For Froude numbers smaller than 1, a rolling regime is evidenced and characterized by avalanches of powders at the free-surface.

For Froude numbers greater than 1, a cataracting regime is observed: the powder is projected when it reaches the surface of the powder bed. However, the great differences in power consumption for the two powders highlight that the flow mechanisms in the powder beds might be completely different.

There is practically no effect of the blade angle on the power consumption for the free-flowing system considered, while it is significant for cohesive powders, especially for high filling ratios in the cataracting regime. This may be confirmed and investigated more into details in future works involving powders of different cohesions. When investigating the effect of the filling ratio on power consumption, a hypothesis on a possible variation of bulk density due to powder compaction under stressing process conditions has been given and may also need confirmation. Correlations between a power number and a Froude number through a simple power law have been established for free-flowing and cohesive powders. These relations involve two coefficients depending on the powder type (coefficient *a*) and on the flow regime considered (coefficient *b*) and are in good agreement with previous work.

In future work, we will focus on the influence of different configurations of blades, vessel and wall position, or vessel inclination, as well as combinations of these. This will give more insight into the flow mechanisms at play, especially for cohesive systems.

Acknowledgments

We would like to thank Asma Toualoua and Luana Grillet, internship students in our laboratory, for their help during rheology measurements that are presented in this work. Many thanks to Pierre Bertorelle for his technical ideas and dedication, both necessary for the elaboration of the blending prototype.

References

André, C., and J. F. Demeyre. 2012. Dimensional analysis of a planetary mixer for homogenizing of free flowing powders: Mixing time and power consumption. *Chemical Engineering Journal* 198–199:371–78. doi:10.1016/j.cej.2012.05.069

André, C., J. F. Demeyre, C. Gatumel, H. Berthiaux, and G. Delaplace. 2014. Derivation of dimensionless relationships for the agitation of powders of different flow behaviours in a planetary mixer. *Powder Technology* 256:33–38. doi:10.1016/j.powtec.2014.02.002.

Bagster, D. F., and J. Bridgewater. 1967. The measurement of the force needed to move blades through a bed of cohesionless granules. *Powder Technology* 1:189–98. doi:10.1016/0032-5910(67)80036-6

Bagster, D. F., and J. Bridgewater. 1969. The flow of granular material over a moving blade. *Powder Technology* 3:323–38. doi:10.1016/0032-5910(69)80104-X

Boonkanokwong, V., B. Remy, J. G. Khinast, and B. J. Glasser. 2016. The effect of the number of impeller blades on granular flow in a bladed mixer. *Powder Technology* 302:333–49.

Carr, R. L. 1965 (January 18). Evaluating flow properties of solids. *Chemical Engineering* 72:163–68.

Cavinato, M., R. Artoni, M. Bresciani, P. Canu, and A. Santomaso. 2013. Scale-up effects on flow patterns in the high shear mixing of cohesive powders. *Chemical Engineering Science* 102:1–9.

Chandratilleke, G. R., A. B. Yu, and J. Bridgwater. 2012. A DEM study of the mixing of particles induced by a flat blade. *Chemical Engineering Science* 79:54–74. doi:10.1016/j.ces.2012.05.010

Chandratilleke, G. R., A. B. Yu, R. L. Stewart, and J. Bridgwater. 2009. Effects of blade rake angle and gap on particle mixing in a cylindrical mixer. Powder Technol., Special Issue: Discrete Element Methods: The 4th International conference on Discrete Element Methods The 4th International Conference on Discrete Element Methods, Brisbane, August 2007, Vol. 193, 303–11. doi:10.1016/j.powtec.2009.03.007

Cleary, P. W. 2013. Particulate mixing in a plough share mixer using DEM with realistic shaped particles. *Powder Technology* 248:103–20. doi:10.1016/j.powtec.2013.06.010

Conway, S. L., A. Lekhal, J. G. Khinast, and B. J. Glasser. 2005. Granular flow and segregation in a four-bladed mixer. *Chemical Engineering Science* 60:7091–107. doi:10.1016/j.ces.2005.03.008

Demeyre, J.-F. 2007. Caractérisation de l'homogénéité de mélange de poudres et de l'agitation en mélangeur Triaxe®. Thèse de doctorat. Institut National Polytechnique.

Halidan, M., G. R. Chandratilleke, S. L. I. Chan, A. B. Yu, and J. Bridgwater. 2014. Prediction of the mixing behaviour of binary mixtures of particles in a bladed mixer. *Chemical Engineering Science* 120:37–48. doi:10.1016/j.ces.2014.08.048

Havlica, J., K. Jirounkova, T. Travnickova, and M. Kohout. 2015. The effect of rotational speed on granular flow in a vertical bladed mixer. *Powder Technology* 280:180–90. doi:10.1016/j.powtec.2015.04.035

Knight, P. C., J. P. K. Seville, A. B. Wellm, and T. Instone. 2001. Prediction of impeller torque in high shear powder mixers. *Chemical Engineering Science* 56:4457–471. doi:10.1016/S0009-2509(01)00114-2

Laurent, B. F. C., and J. Bridgwater. 2002. Influence of agitator design on powder flow. *Chemical Engineering Science* 57:3781–793. doi:10.1016/S0009-2509(02)00317-2

Laurent, B. F. C., and P. W. Cleary. 2012. Comparative study by PEPT and DEM for flow and mixing in a ploughshare mixer. *Powder Technology* 228:171–86. doi:10.1016/j.powtec.2012.05.013

Legoix, L., C. Gatumel, M. Milhé, and H. Berthiaux. 2017. Rheology of cohesive powders in a pilot scale planetary blender, *Powder Technology* 305:609–19.

Leturia, M., M. Benali, S. Lagarde, I. Ronga, and K. Saleh. 2014. Characterization of flow properties of cohesive powders: A comparative study of traditional and new testing methods. *Powder Technology* 253:406–23. doi:10.1016/j.powtec.2013.11.045

Makishima, S.-I., and T. Shirai. 1968. Experimental study on the power requirements for agitating beds of solid particles, and proposal of a new model. *Journal of Chemical Engineering of Japan* 1:168–74. doi:10.1252/jcej.1.168

Malhotra, K., A. S. Mujumdar, and M. Miyahara 1990a. Estimation of particle renewal rates along the wall in a mechanically stirred granular bed. *Chemical Engineering and Processing: Process Intensification* 27:121–30. doi:10.1016/0255-2701(90)87001-Y

Malhotra, K., A. S. Mujumdar, and M. Okazaki. 1990b. Particle flow patterns in a mechanically stirred two-dimensional cylindrical vessel. *Powder Technology* 60:179–89. doi:10.1016/0032-5910(90)80142-L

Malhotra, K., A. S. Mujumdar, H. Imakoma, and M. Okazaki. 1988. Fundamental particle mixing studies in an agitated bed of granular materials in a cylindrical vessel. *Powder Technology* 55:107–14. doi:10.1016/0032-5910(88)80093-7

Malhotra, K., and A. S. Mujumdar. 1990. Particle mixing and solids flowability in granular beds stirred by paddle-type blades. *Powder Technology* 61:155–64. doi:10.1016/0032-5910(90)80150-W

Mayer-Laigle, C. 2012. Étude dynamique et effet du changement d'échelle pour plusieurs systèmes particulaires en mélangeur Turbula®: Application à un mélange destiné à la fabrication de plaques composites. Thèse de doctorat. Institut National Polytechnique.

Mellmann, J. 2001. The transverse motion of solids in rotating cylinders—forms of motion and transition behavior. *Powder Technology* 118:251–70. doi:10.1016/S0032-5910(00)00402-2

Moakher, M., T. Shinbrot, and F. J. Muzzio 2000. Experimentally validated computations of flow, mixing and segregation of non-cohesive grains in 3D tumbling blenders. *Powder Technology* 109: 58–71. doi:10.1016/S0032-5910(99)00227-2

Radl, S., D. Brandl, H. Heimburg, B. J. Glasser, and J. G. Khinast. 2012. Flow and mixing of granular material over a single blade. *Powder Technology* 226:199–12. doi:10.1016/j.powtec.2012.04.042

Remy, B., J. G. Khinast, and B. J. Glasser 2011. Polydisperse granular flows in a bladed mixer: Experiments and simulations of cohesionless

spheres. *Chemical Engineering Science* 66: 1811–824. doi:10.1016/j.ces.2010.12.022

Remy, B., T. M. Canty, J. G. Khinast, and B. J. Glasser. 2010. Experiments and simulations of cohesionless particles with varying roughness in a bladed mixer. *Chemical Engineering Science* 65:4557–571. doi:10.1016/j.ces.2010.04.034

Siraj, M. S. 2014. Single-blade convective powder mixing: The effect of the blade shape and angle. *Powder Technology* 267:289–301. doi:10.1016/j.powtec.2014.07.024

Zhou, Y. C., A. B. Yu, R. L. Stewart, and J. Bridgwater. 2004. Microdynamic analysis of the particle flow in a cylindrical bladed mixer. *Chemical Engineering Science* 59:1343–364. doi:10.1016/j.ces.2003.12.023